Digital Discovery

ROYAL SOCIETY OF CHEMISTRY

PAPER

View Article Online
View Journal | View Issue

Cite this: *Digital Discovery*, 2026, **5**, 1363

A mobile robotic process chemist

Emma J. Brass, Satheeshkumar Veeramani, Zhengxue Zhou, Hatem Fakhruldeen, J. Sebastian Manzano, Rob Clowes, Isil Akpinar, Miriam R. Ward, John W. Ward * and Andrew I. Cooper *

Received 16th December 2025
Accepted 22nd February 2026

DOI: 10.1039/d5dd00563a

rsc.li/digitaldiscovery

Process chemistry creates scalable routes for new lead molecules and is a crucial but laborious stage in pharmaceutical and agrochemical development cycles. We have built an automated process chemistry platform that tackles late-stage process development. The modular workflow integrates both industry-standard tools and bespoke devices to enable process scale synthesis, work-up, and analysis. A multitasking mobile robot works between an automated synthesis reactor and an ultra-high-performance liquid chromatography-mass spectrometer (UHPLC-MS) for product analysis, cleaning the reactor between runs. The robot's anthropomorphic manipulation capabilities allow it to interface with minimally redesigned equipment that can be shared with human researchers. Reaction yields and purity match human chemist performance. Timings for round-the-clock, back-to-back experiments suggest that the weekly reaction output of the robot operating multiple reactors could exceed that of a human process chemist by a factor of 12 in an industrial setting.

Process development is a vital but resource intensive stage in pharmaceutical and agrochemical development pipelines. Process chemists are concerned with optimizing a synthetic pathway to prepare for scale-up to pilot plant production. Early-stage process chemistry is typically conducted on a small scale (<20 mL reaction volume) using arrays of vials or small reactors in automated synthesis platforms, a method often referred to as high-throughput experimentation (HTE).[1–4] This allows for screening reaction parameters such as solvent, catalyst, or reaction temperature to optimize a reaction pathway. This resembles the methods used in discovery chemistry, where HTE is used to screen compound libraries against therapeutic targets.[5–9] Once reaction optimization has taken place, late-stage process chemistry is concerned with ensuring process safety and robustness,[10] often using structured experimental methodologies such as design of experiments.[11,12] Late-stage process chemistry is typically carried out on a much larger scale in 500 mL to 5 L reactors that more closely mimic pilot plant reactors. It is far more challenging to create reactor arrays at this scale, and hence sequential manual reactions with one scientist per reactor has been the prevailing paradigm over the last 50 years. This is a laborious process, as experiments are often repeated multiple times with only small variations between conditions. Such repetition is necessary to enable deep interrogation of a system, to generate the dense datasets needed to support safe scale-up. Also, while flow reactors are widely used in early-stage process chemistry and reaction optimization,[13,14] they are less amenable to late-stage process chemistry for reactions that will later be scaled up in batch.

Automated platforms for discovery chemistry and early-stage process chemistry exist both as commercially available products (*e.g.*, Chemspeed, Unchained Labs) and as prototypes developed by academic groups.[15–19] Recently, we developed a 'mobile robotic chemist'—that is, a mobile robotic manipulator that can be used to carry out both catalysis research[20] and small-scale exploratory synthesis.[21] An advantage of this approach is that the mobile robotic chemist can operate existing laboratory instrumentation that was designed for human use without significant modifications—it is a potential drop-in solution. However, this mobile robotic chemist was developed for photocatalysis and exploratory synthesis research on a scale (<100 mL) that is unsuitable for late-stage process chemistry.

Here we present a modular automated robotic platform for general late-stage process chemistry. We tackled key operations including synthesis, work-up (filtration), product analysis, product weighing, and reactor cleaning (Fig. 1). We chose the synthesis of paracetamol (*N*-(4-hydroxyphenyl)ethanamide) because it involves many of the unit operations used in late-stage process chemistry, such as liquid and solid dispensing, heating and cooling, stirring, filtration, chromatographic analysis, and product weighing. Given the larger scale (1000 mL reaction volume), this aqueous synthesis also provided a safe platform for development of a fully automated workflow. The mobile robotic chemist approach allowed us to build a workflow using commercially available laboratory equipment, in some cases with no physical modifications. Where immediate integration was not possible, modifications were made using cost-

Department of Chemistry and Materials Innovation Factory, University of Liverpool, Liverpool, L7 3NY, UK. E-mail: aicooper@liverpool.ac.uk; john.ward@liverpool.ac.uk

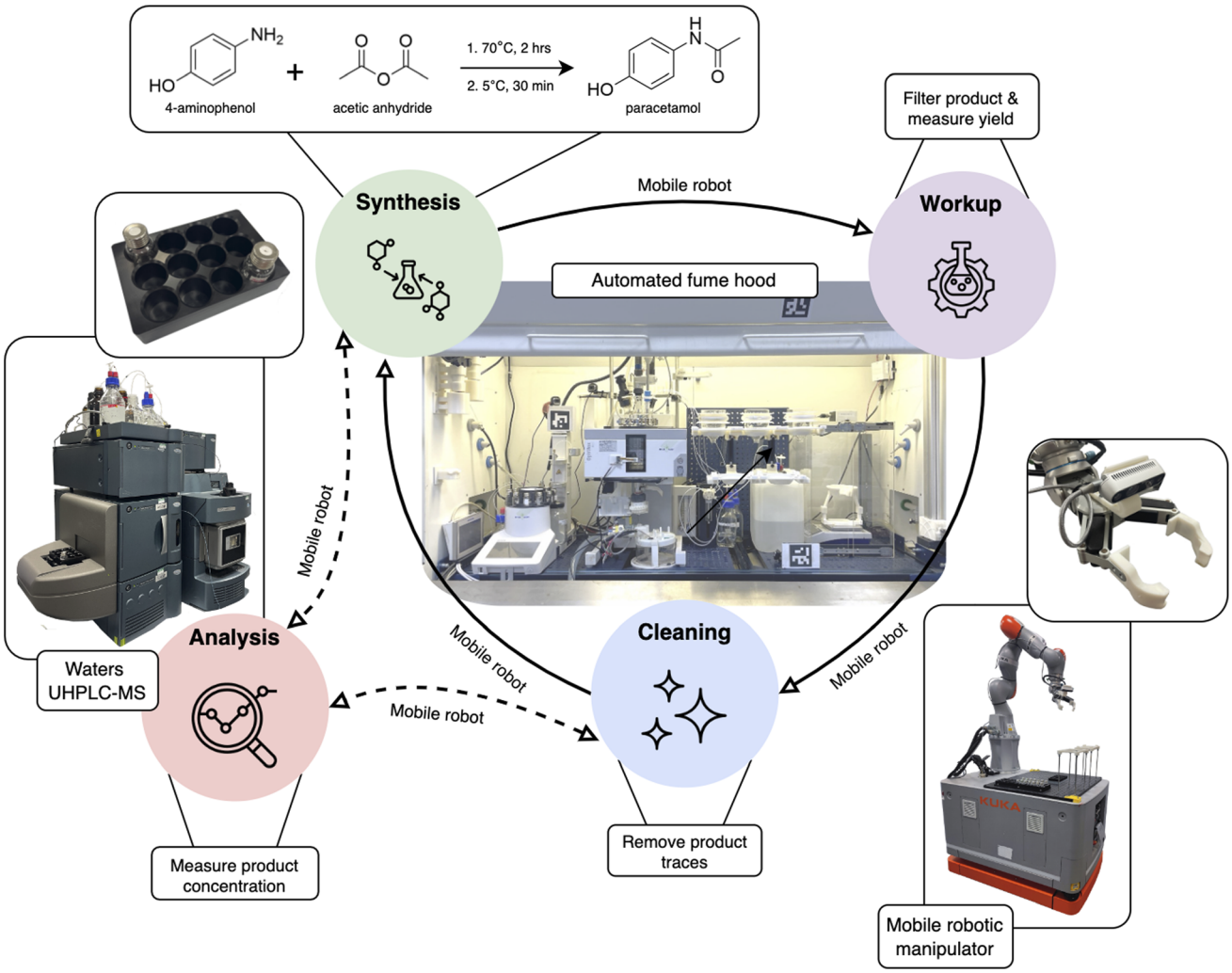

Fig. 1 Process chemistry workflow that automates synthesis, work-up, and reactor cleaning steps, allowing for multiple consecutive reaction runs. The synthesis and work-up steps make use of both commercial and custom-made equipment. Chromatographic analysis was performed both during synthesis and to validate the cleaning steps. A general purpose mobile robotic manipulator was used for all manipulation and transportation tasks, avoiding the need for multiple robotic arms.

effective solutions that involved 3D printing, motors and valves, and inexpensive microcontrollers.

Automated process chemistry platform

The commercially available equipment and bespoke devices built for this workflow are shown in Fig. 2. The equipment in the fume cupboard was fixed in precise, savable locations using a breadboard. The key operations in the workflow are as follows.

Fume hood operation

Two methods were used to allow the mobile robotic manipulator access into the fume hood. To access the autosampler samples and the solid dispensing devices (Fig. 2b and e), the robot grasps a 3D printed handle to open the horizontal sliding sash (*e.g.*, Supporting Video M1, timestamp 0′39″). For filter funnel manipulations, the whole sash was opened vertically using a motorized actuator fixed to the inside wall of the fume hood (*e.g.*, Supporting Video M1, timestamp 0′12″). This allows the robot to access the relevant equipment while minimizing disruption to extraction in the fume hood.

Reaction chemistry

Process chemists typically use controlled lab reactors (CLR), which are jacketed cylindrical glass vessels with accurate control over heating and stirring rate. A 1000 mL Mettler Toledo OptiMax reactor was used here.[22–24] This is an industry standard item that is commonly used in pharmaceutical process chemistry laboratories. The reactor was automated using the supplied iControl software.

Liquid dispensing

Liquid reagent addition was carried out using a Tecan Cavro XLP 6000 syringe pump with a 12-port ceramic valve, PTFE

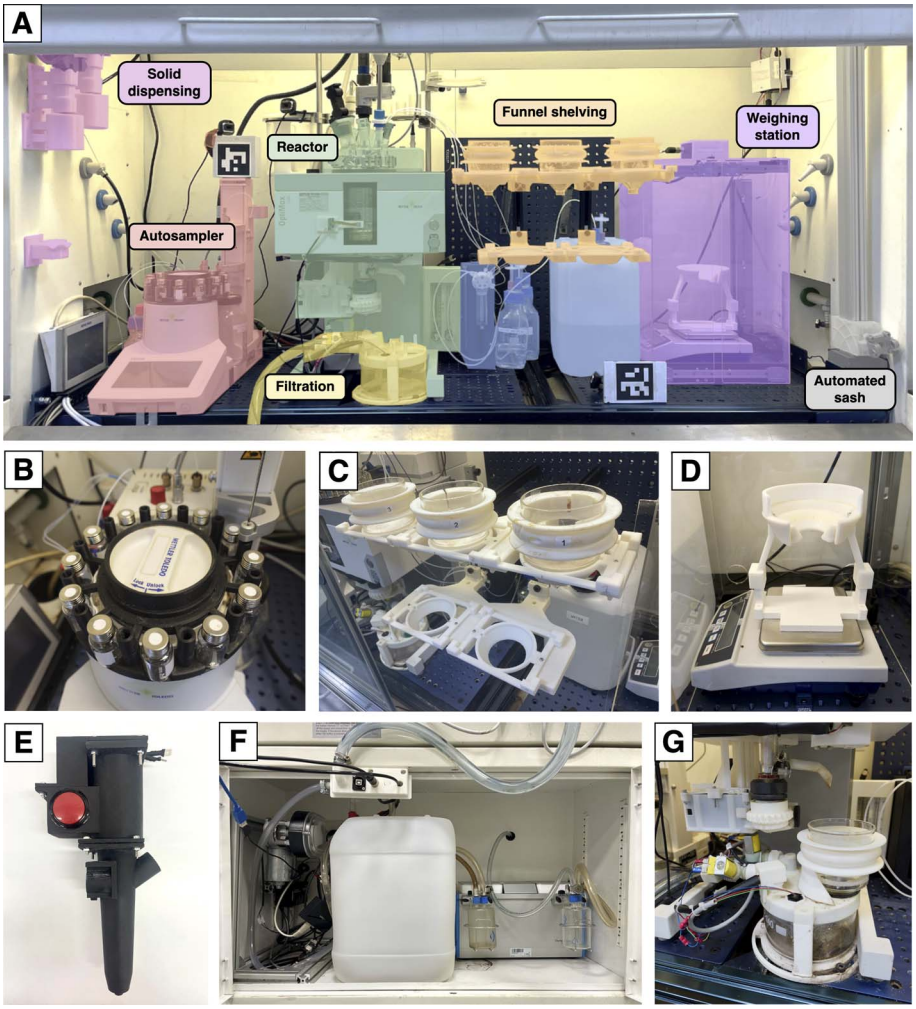

Fig. 2 Automated process chemistry platform. (a) Photograph of a standard-sized fume hood with the various key components highlighted. (b) Close up photograph of the autosampler, showing the modified vial carousel. (c) Shelves holding three filtration funnels. (d) Balance with a funnel holder fixed on the weighing pan. (e) Custom-built solid dispensing device. (f) Solvent cupboard underneath the fume hood housing the peristaltic pump for draining filtrate (left), a 20 L jerry can for collecting waste filtrate (middle), and the vacuum pump for filtration (right). (g) Automated reactor base valve situated above the filtration system, shown with a Büchner funnel in place.

tubing, and a 25 mL syringe (*e.g.*, Supporting Video M1, timestamp 0′31″).

Solid dispensing

Process chemistry typically involves the addition of solid reagents on gram to kilogram scale. This workflow required a solid dispensing device that could add 20 g of solid 4-aminophenol powder directly into the Mettler Toledo reactor. We found that commercially available solid-dosing devices were not able to meet these criteria. We therefore designed and built a device (Fig. 2a and e and Supplementary Fig. 1) that can be pre-loaded and operated by the mobile robot in the workflow. The robot inserts this device into one of the ground glass side ports of the reactor and then operates it to add the solid with a physical button press (Supporting Video M1, timestamp 0′46″). In principle, this pre-loaded solid dispenser could be used by a human operator in the same way. When not in use, the cartridge sits in a holder attached to the fume hood wall (Supplementary Fig. 1c).

Reaction analysis

A commercial Mettler Toledo EasySampler was used for sampling from the reactor. Samples were stored in 10 mL vials located on a vial carousel. The original vial carousel did not allow enough space around the vial caps for the mobile robot to grasp, hence we adapted this with a 3D printed version. Analysis of reaction progress was conducted on a Waters ultra-high-performance liquid chromatography-mass spectrometer (UHPLC-MS) using caffeine as an internal standard, and a heuristic decision-maker was developed to process the data. As is standard in most industrial R&D laboratories, the UHPLC-MS was in a separate area of the laboratory, requiring samples to be transported by the robot (Supporting Video M1, timestamp 1′41″–2′20″). This has advantages over direct sampling since UHPLC-MS instruments are expensive, and invariably shared between multiple process chemistry reactors.

Product recovery and filtration

The Mettler Toledo OptiMax reactor has a manual-operation base valve. To automate this valve, we mounted a stepper motor perpendicular to the valve, with a worm gear for coupling the valve handle to the motor. We developed a filtration system to sit underneath the base valve (Fig. 2a and g). This consists of a glass dish covered by a 3D printed lid with a conical depression for a 250 mL sintered glass funnel to sit in (Supporting Video M1, timestamp 3′31″). The lid has a connection to vacuum and a connection to a peristaltic pump for waste drainage, both regulated by solenoid valves.

Weighing

A Kern PCB 2500-2 balance was used for weighing the reaction product. A custom-built enclosure prevented weighing errors arising from fume hood air flow. A 3D printed funnel holder was added to the balance pan (Supporting Video M1, timestamp 4′11″).

Reactor cleaning

To allow sequential reactions and continuous round-the-clock operation, the reactor must self-clean. In the cleaning stages, a concentration of 0.05 mg mL^{-1} (*N*-(4-hydroxyphenyl)ethanamide) was chosen as the upper threshold for cleaning to be considered complete. The system was also programmed to do at least two cleaning cycles, even if the paracetamol concentration was deemed to be below this threshold after the first cleaning sample (Supporting Video M1, timestamp 4′33″–6′31″).

Mobile robot chemist

We showed previously that free-roaming mobile robots could be integrated into existing laboratories to perform experiments by emulating the physical operations of human scientists;[20,21,25] other laboratories have also embraced this approach.[26,27] In this workflow, fiducial markers were used to compensate for error in the base positioning and to accurately localize the robot end effector, rather than the 6-point calibration used previously.[20,21,25] This visual calibration method resulted in a translation precision of ±0.41 mm and a rotational precision of ±1.014°. While this method exhibits slightly lower translational and rotational accuracy than the previously used 6-point calibration, the achieved precision is sufficient for reliable task execution within the context of this workflow. This method also offers practical advantages; it requires only visual access to the calibration target from a distance, rather than physical access to all faces of a calibration cube *via* direct gripper contact. This reduces constraints on target placement and simplifies integration within confined laboratory environments.

The mobile base of the robot was used to store objects for transportation (Supplementary Fig. 3). We fitted a short rack for holding the sample vial that was being transported, a long rack for storing sample vials after they have been analyzed, and a raised holder for a hollow funnel that is used during cleaning.

The mobile base unit allows the robot arm to be used anywhere in the laboratory. In this workflow, the robot is positioned on the right side of the fume hood to move funnels between the shelves, and to operate the filtration system and the weighing station. It moves to the left side of the fume hood

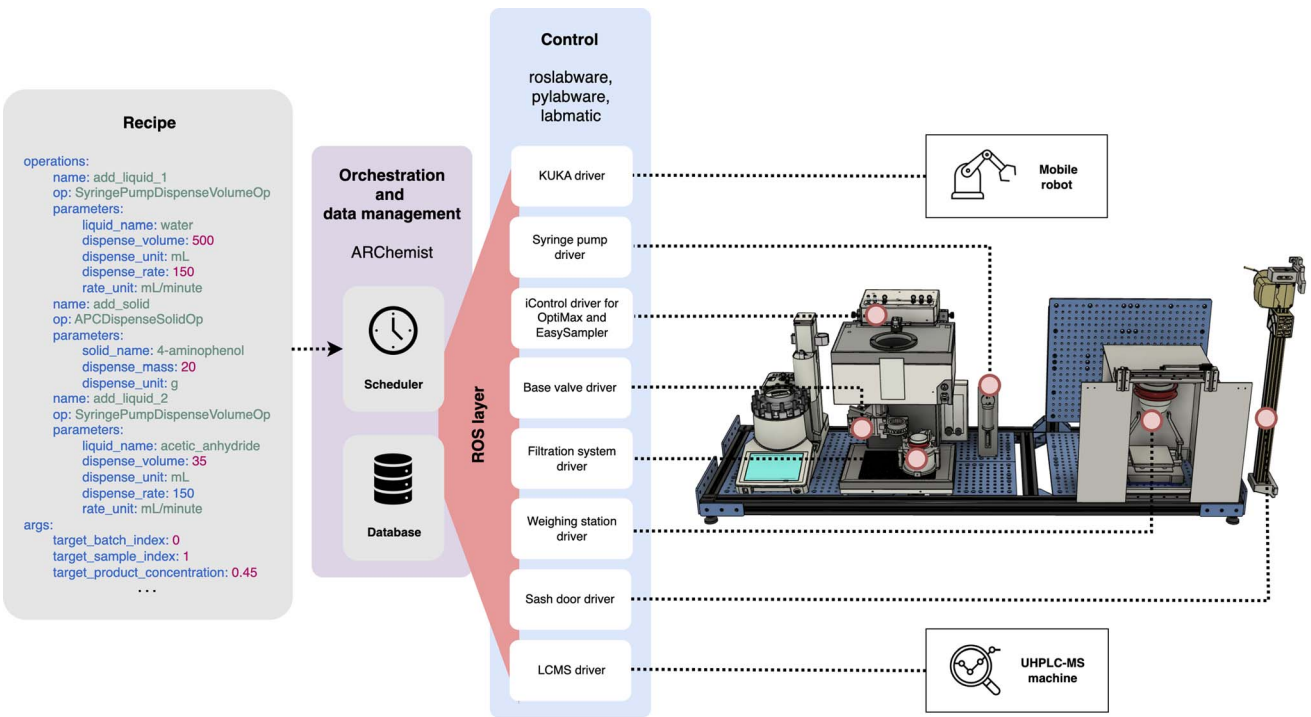

Fig. 3 Software overview. ARChemist takes a human-readable recipe file as the input and handles high-level orchestration and data management. Roslabware, pylabware, and labmatic packages handle low-level control and send commands out to individual devices.

when manipulating the solid dispensing device or collecting sample vials. It then drives across the lab to drop off sample vials for analysis on the UHPLC-MS machine. This approach is highly scalable and flexible, since the instruments and fume hoods can be located anywhere in the laboratory. While such integrations might be also achieved with robots on tracks,[28–30] this would increase costs, consume space, and reduce flexibility as the scale of the workflow grows, noting that large industrial R&D labs might contain 20 or more process chemistry reactors, each in a separate fume hood.

A multipurpose robot gripper (Supplementary Fig. 4) was designed to meet the handling requirements for several different objects in the workflow. This included vials, the solid dispensing devices, the fume hood door handle, and filtration funnels. The diameter of the gripper's semicircular internal surface was initially set based on the sample vials, which are standard, fixed consumable items. The fume hood door handle, funnel handles, and solid dispensing device handles were then designed based on those gripper dimensions.

Software

Orchestration of the workflow required robust software with multiple levels of abstraction and control. Fig. 3 gives an overview of the software architecture.

ARChemist is a modular architecture for workflow orchestration and data management based on the Robot Operating System (ROS)[31] that was designed to be simple to use for a scientist with limited coding knowledge. The scientist uses intuitive chemical procedures in the form of YAML files to program their automated experimental setup. ARChemist sends out commands at the correct time and in the correct order to request processes to take place within the workflow; it stores the status of each process in a MongoDB database for viewing at any time.

Pylabware provides Python functions that abstract away the details of each device's unique communication protocol.[32] Roslabware wraps around pylabware and allows these devices to be controlled over the lab network using ROS messages sent from ARChemist. ROS is an open-source middleware that is commonplace in robotic systems.[33]

Most devices used simple communication protocols such as serial commands. Automating the reactor and autosampler through Mettler Toledo's proprietary iControl software required the use of GUI automation. The labmatic package for automating the Waters UHPLC-MS machine creates a CSV file that is sent to the UHPLC-MS software. This triggers startup of the machine and analysis of the sample. The output file is parsed by labmatic. It assigns peaks by comparing peak maxima to predetermined retention times for compounds expected to be found in the sample.

Experimental procedure

The experimental procedure is summarized in Fig. 4. First, a chemist performed an initial set up that included placing clean funnels on the shelves, ensuring the autosampler is fully loaded with clean vials, and loading the solid dispensing cartridges. All operations were then conducted without manual intervention, up to and including weighing the final product. After the automated runs, the chemist would shut down the system by turning off power supplies and moving the paracetamol product from the funnels into storage vessels.

The mobile robot began by moving a funnel to the filtration system. The syringe pump dispensed 500 mL of distilled water into the reactor and the mobile robot operated a solid dispensing device to add 20 g of 4-aminophenol. The reactor was heated to 70 °C, then the autosampler withdrew a 20 μL sample. After the first sample, 35 mL of acetic anhydride was pumped into the reactor. The mobile robot transferred the sample to the UHPLC-MS machine for analysis, whereby a decision was made based on the results. If the concentration was above 0.45 mg mL^{-1}—a predetermined target reaction yield—then the system moved on to workup. If not, the reactor continued to heat, and the robot returned to collect another sample. In-experiment UHPLC-MS data is shown in the SI.

Workup began with cooling the reactor to 5 °C to initiate product crystallization. The base valve was operated in four open/close cycles to drain slurry down into the funnel. Vacuum was applied, then the drain peristaltic pump was turned on to move waste filtrate to the 20 L jerrycan under the fume hood. When the reactor was empty, it was refilled again with water, stirred, and drained to remove any residual paracetamol from the inside surfaces. Finally, vacuum was applied for 5 minutes to dry out the paracetamol product. The mobile robot moved the funnel to the balance for product mass measurement, then returned it to the shelves.

In the cleaning phase, a hollow funnel with no frit was placed on the filtration system. The reactor was filled with 600 mL distilled water, then heated to 85 °C. Again, a sample was transferred to the UHPLC-MS for analysis. The paracetamol concentration in the sample needed to be below 0.05 mg mL^{-1} for it to be considered clean. Furthermore, at least two samples were required before the cleaning stage was finished. Once this was achieved, the hollow funnel was moved back to the mobile robot base, to ready the system for the next reaction.

A video of the whole experimental procedure is included in the SI (Movie 1).

Results

After building the system, there was an initial period of running individual experiments while debugging the software and improving the bespoke hardware (SI, Supplementary Table 2). We then moved to running the system continuously to demonstrate the principle of round-the-clock automation. We carried out three consecutive paracetamol syntheses over a period of 21 h (SI, Movie 2) and obtained consistent recovered product yields (15.80 g, 15.72 g, 15.80 g; corresponding to percentage yields of 57.0%, 56.8%, 57.0%). NMR data (SI, Supplementary Fig. 7) confirmed high purity of the paracetamol product in all cases. To benchmark the robot performance, we performed an analogous manual synthesis of paracetamol,

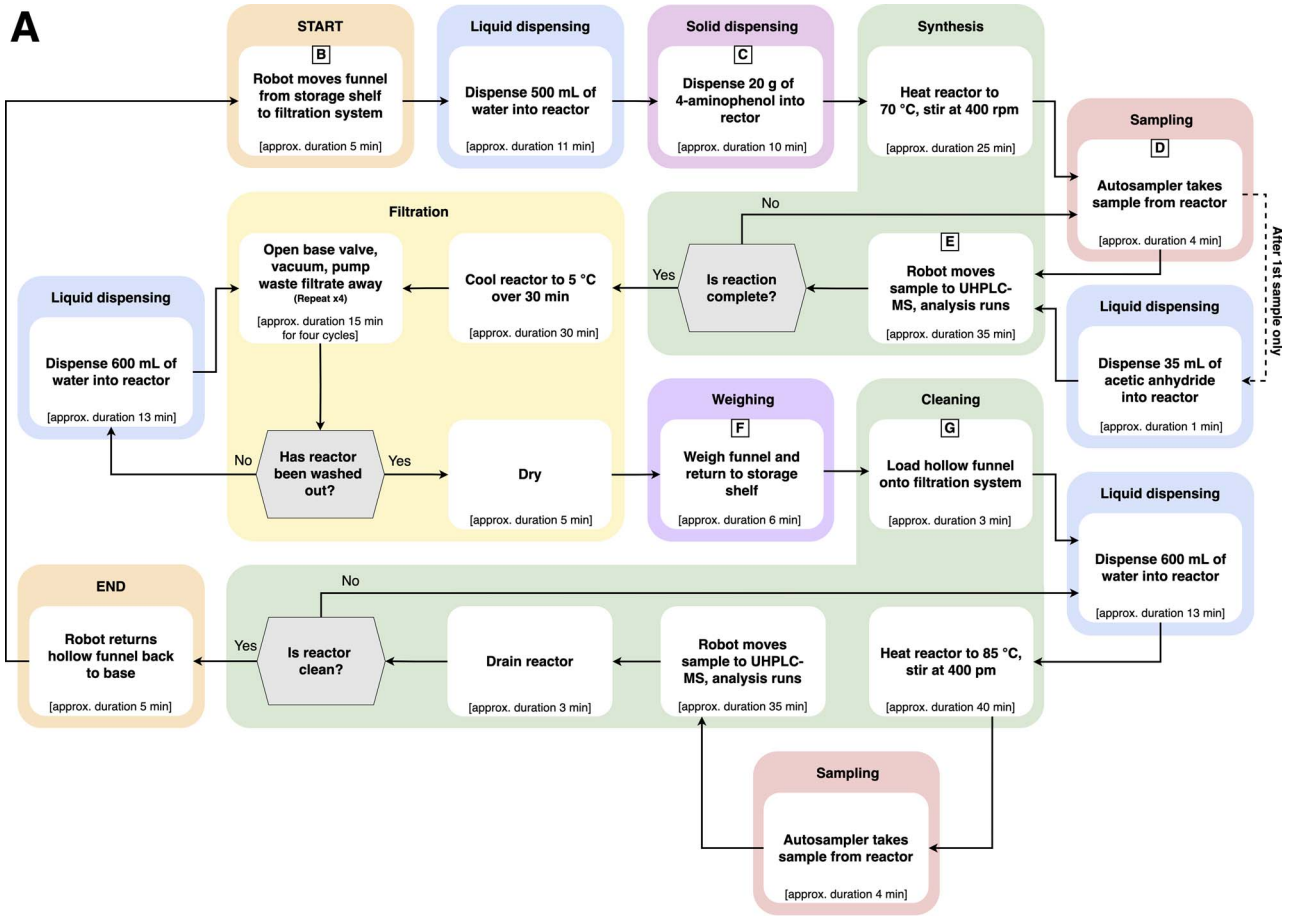

Fig. 4 Key steps in the automated process chemistry workflow. (a) First, the robot moves a funnel to the filtration system and then continues as shown, following the arrows. Hexagonal blocks are decision points. The average duration for each step is shown in square brackets. The colors of each step correspond to the equipment coloration in Fig. 2. (b) Robot lifting a funnel off the storage shelves. (c) Robot pressing the button to dispense solid into the reactor. (d) Robot removing a sample vial from the autosampler. (e) Robot placing a sample vial on the UHPLC-MS vial rack. (f) Robot placing a funnel of the balance for yield measurement. (g) Robot picking up the hollow funnel from its base for placement on the filtration system.

achieving an average recovered product yield of 59.9% following the same procedure.

These three experiments ran over a continuous period of 20 hours 52 minutes, averaging approximately 7 hours per experiment, including synthesis, product isolation, analysis, and reactor cleaning. Assuming longer-term workflow stability and 24/7 operation, then 24 consecutive experiments per week could be carried out by the system for this benchmark reaction. With no interruptions or breaks, a human researcher can perform this experiment in around 3 hours, based on our control experiments—that is, faster than the mobile robot. The robot moves relatively slowly for safety reasons, meaning that the human researcher has a speed advantage in manipulation and laboratory navigation tasks. Nonetheless, in a realistic work scenario, a human chemist working a 40 hour, 5 day week with a single reactor could conduct two of these experiments per day; one in the morning and one in the afternoon. This equates to 10 experiments per week, compared to the 24 experiments that the robot could achieve. Moreover, as shown by Movie 2, the mobile robot is far from capacity in this workflow. It operates for only 20% of the run time, on average, spending most of that time waiting for other operations to complete. As such, with smart scheduling and allowing for battery recharges, a single mobile robotic manipulator might serve around five such reactors. This could allow one mobile robot to complete 120 reactions per week, exceeding the reaction output of a single human process chemist by a factor of 12.

Outlook

Unlike discovery chemistry and early-stage process chemistry, late-stage process chemistry has so far resisted automation. It is challenging to create arrays of fully automated reactors, each of which occupies a standard fume hood (Fig. 2a), coupled with appropriate analytical steps. Here we show that mobile robots can be used to integrate the basic unit operations in late-stage process chemistry, replicating the performance of a human process chemist, for the simple case of paracetamol synthesis. These preliminary experiments suggest that such automated systems could exceed the reaction output of a human process chemist by more than a factor of ten, even though the completion of an individual experiment by the robot is slower. This speed up is because robots can operate 24/7 and focus exclusively on process chemistry tasks with no distractions. To achieve such productivity gains, and to ensure safety, it would be necessary to improve the workflow robustness. We demonstrate here three back-to-back experiments over the course of 21 hours with no failures (SI, Movie 2). However, this required extensive optimization and fine-tuning of the workflow. The 24/7, five reactor scenario that we invoke above is beyond the capabilities of the current set up. This is because of the open-loop nature of the workflow. Greater robustness could be achieved by including active feedback, for example to detect whether an item has been slightly misplaced by the robot and to take appropriate corrective action. Likewise, we demonstrate this method with a well-known reaction. More conditional logic might be required for new reactions, for example to determine the appropriate course of action if the product does not precipitate out, as anticipated. Furthermore, while the present system provides access to standard process data *via* iControl (*e.g.*, temperature, volume, and stirring rate), it does not yet incorporate the full suite of data-rich kinetic and thermal analyses that typically guide safe industrial scale-up decisions. Future extensions could integrate additional process-chemistry instrumentation—such as *in situ* spectroscopic probes, reaction calorimetry, and higher-frequency automated sampling—to support kinetic interpretation and thermal risk assessment in a more industrially representative context.

We believe that modular integration using industrial mobile robots[34] will have economic advantages over physically integrated automation solutions, particularly at the process chemistry scale. For example, the UHPLC-MS instrument in this workflow is more expensive than either the mobile robot or the reactors, and hence it is much more cost-effective to share this analytical hardware between reactors, rather than hard-wiring it to a single reactor. We have also shown that other key analytical techniques, such as NMR, can be incorporated using mobile robots.[21]

In the experiments described here, the decision making is simple and hard-coded, allowing the system to determine when the reaction is complete, or whether the reactor is clean enough for the next experiment (Fig. 4a). In the future, we foresee the introduction of more advanced artificial intelligence: for example, to allow the autonomous optimization of reaction conditions to maximize yield or product purity at this late-stage process chemistry scale.

Author contributions

Conceptualization: M.R.W., J.W.W., A.I.C.; data curation: E.J.B.; formal analysis: E.J.B., S.V., funding acquisition: M.R.W., J.W.W., A.I.C., investigation: E.J.B., S.V., Z.Z., H.F., methodology: E.J.B., S.V., Z.Z., H.F., J.S.M., R.C., J.W.W., A.I.C.; project administration: H.F., I.A, M.R.W., J.W.W., A.I.C.; resources: E.J.B.; software: E.J.B., S.V., Z.Z., H.F., J.S.M.; supervision: H.F., J.W.W., A.I.C.; validation: E.J.B., S.V., Z.Z.; visualization: E.J.B., S.V., Z.Z., H.F., M.R.W., J.W.W., A.I.C.; writing: E.J.B., J.W.W. A.I.C., S.V., H.F., I.A.

Conflicts of interest

Authors declare that they have no competing interests.

Data availability

References 35–37 are cited in the Supplementary information (SI). UHPLC-MS data for each experiment and product NMR data have been deposited on Zenodo under a CC-BY-SA 4.0 license at https://doi.org/10.5281/zenodo.15625410.

Supplementary information: Movies S1 and S2 are available on YouTube at the following links: https://www.youtube.com/watch?v=XdxzEjBgC0Q, https://www.youtube.com/watch?v=Pvdyf3zxtlk. See DOI: https://doi.org/10.1039/d5dd00563a.

Design file availability

CAD files for 3D printed pieces have been deposited on Zenodo under a CC-BY-SA 4.0 license at https://doi.org/10.5281/zenodo.15756523.

Code availability

Workflow orchestration code in ARChemist has been deposited on GitHub under an MIT License at https://github.com/cooper-group-uol-robotics/archemist/tree/apc_handlers. All other code has been deposited on Zenodo under an MIT License at https://doi.org/10.5281/zenodo.15756809.

Acknowledgements

The authors thank GSK, AstraZeneca, Syngenta, and Pfizer for co-funding this work. We thank Dr Ehsan Simaei, who designed and constructed the filtration system, the waste handling unit, and the balance enclosure. The authors also received funding from the Leverhulme Trust *via* the Leverhulme Research Centre for Functional Materials Design. The project was also supported by the Engineering and Physical Sciences Research Council (EPSRC, EP/V026887). AIC thanks the Royal Society for a Research Professorship (RSRP\S2\232003). We also thank Mettler Toledo for the provision of their OptiMax and Easy-Sampler platforms.

Notes and references

1 J. A. Selekman, J. Qiu, K. Tran, J. Stevens, V. Rosso, E. Simmons, Y. Xiao and J. Janey, High-throughput automation in chemical process development, *Annu. Rev. Chem. Biomol. Eng.*, 2017, **8**, 525–547.

2 S. M. Mennen, C. Alhambra, C. L. Allen, M. Barberis, S. Berritt, T. A. Brandt, A. D. Campbell, J. Castañón, A. H. Cherney, M. Christensen, D. B. Damon, J. E. de Diego, S. García-Cerrada, P. García-Losada, R. Haro, J. Janey, D. C. Leitch, L. Li, F. Liu, P. C. Lobben, D. W. C. MacMillan, J. Magano, E. McInturff, S. Monfette, R. J. Post, D. Schultz, B. J. Sitter, J. M. Stevens, I. I. Strambeanu, J. Twilton, K. Wang and M. A. Zajac, The evolution of high-throughput experimentation in pharmaceutical development and perspectives on the future, *Org. Process Res. Dev.*, 2019, **23**, 1213–1242.

3 V. Rosso, J. Albrecht, F. Roberts and J. M. Janey, Uniting laboratory automation, DoE data, and modeling techniques to accelerate chemical process development, *React. Chem. Eng.*, 2019, **4**, 1646–1657.

4 J. P. McMullen and J. A. Jurica, Accelerating reaction optimization through data-rich experimentation and machine-assisted process development, *React. Chem. Eng.*, 2024, **9**, 2160–2170.

5 S. W. Krska, D. A. DiRocco, S. D. Dreher and M. Shevlin, The evolution of chemical high-throughput experimentation to address challenging problems in pharmaceutical synthesis, *Acc. Chem. Res.*, 2017, **50**, 2976–2985.

6 B. Mahjour, Y. Shen and T. Cernak, Ultrahigh-throughput experimentation for information-rich chemical synthesis, *Acc. Chem. Res.*, 2021, **54**, 2337–2346.

7 D. Tiebes and S. Peters, Combinatorial Chemistry, in *Ullmann's encyclopedia of industrial chemistry*, Wiley, 2000.

8 G. Lowe, Combinatorial chemistry, *Chem. Soc. Rev.*, 1995, **24**, 309–317.

9 R. Liu, X. Li and K. S. Lam, Combinatorial chemistry in drug discovery, *Curr. Opin. Chem. Biol.*, 2017, **38**, 117–126.

10 X. Hu, E. Bortell, F. W. Kotch, A. Xu, B. Arve and S. Freese, Development of commercial-ready processes for antibody drug conjugates, *Org. Process Res. Dev.*, 2017, **21**, 601–610.

11 S. A. Weissman and N. G. Anderson, Design of experiments (DoE) and process optimization: A review of recent publications, *Org. Process Res. Dev.*, 2015, **19**, 1605–1633.

12 A. C. F. Cruz, E. M. Mateus and M. J. Peterson, Process development of a Sonogashira cross-coupling reaction as the key step of tirasemtiv synthesis using design of experiments, *Org. Process Res. Dev.*, 2021, **25**, 668–678.

13 P. M. Pittaway, S. T. Knox, O. J. Cayre, N. Kapur, L. Golden, S. Drillieres and N. J. Warren, Self-driving laboratory for emulsion polymerization, *Chem. Eng. J.*, 2025, **507**, 160700.

14 A. M. K. Nambiar, C. P. Breen, T. Hart, T. Kulesza, T. F. Jamison and K. F. Jensen, Bayesian optimization of computer-proposed multistep synthetic routes on an automated robotic flow platform, *ACS Cent. Sci.*, 2022, **8**, 825–836.

15 S. Steiner, J. Wolf, S. Glatzel, A. Andreou, J. M. Granda, G. Keenan, T. Hinkley, G. Aragon-Camarasa, P. J. Kitson, D. Angelone and L. Cronin, Organic synthesis in a modular robotic system driven by a chemical programming language, *Science*, 2019, **363**, eaav2211.

16 J. Liu, Y. Sato, F. Yang, A. J. Kukor and J. E. Hein, An adaptive auto-synthesizer using online PAT feedback to flexibly perform a multistep reaction, *Chem. Methods*, 2022, **2**, e202200009.

17 J. Li, S. G. Ballmer, E. P. Gillis, S. Fujii, M. J. Schmidt, A. M. E. Palazzolo, J. W. Lehmann, G. F. Morehouse and M. D. Burke, Synthesis of many different types of organic small molecules using one automated process, *Science*, 2015, **347**, 1221–1226.

18 B. A. Koscher, R. B. Canty, M. A. McDonald, K. P. Greenman, C. J. McGill, C. L. Bilodeau, W. Jin, H. Wu, F. H. Vermeire, B. Jin, T. Hart, T. Kulesza, S.-C. Li, T. S. Jaakkola, R. Barzilay, R. Gómez-Bombarelli, W. H. Green and K. F. Jensen, Autonomous, multiproperty-driven molecular discovery: From predictions to measurements and back, *Science*, 2023, **382**, eadi1407.

19 C. W. Coley, D. A. Thomas III, J. A. M. Lummiss, J. N. Jaworski, C. P. Breen, V. Schultz, T. Hart, J. S. Fishman, L. Rogers, H. Gao, R. W. Hicklin, P. P. Plehiers, J. Byington, J. S. Piotti, W. H. Green, A. J. Hart, T. F. Jamison and K. F. Jensen, A robotic platform for flow synthesis of organic compounds informed by AI planning, *Science*, 2019, **365**, eaax1566.

20 B. Burger, P. M. Maffettone, V. V. Gusev, C. M. Aitchison, Y. Bai, X. Wang, X. Li, B. M. Alston, B. Li, R. Clowes,

N. Rankin, B. Harris, R. W. Sprick and A. I. Cooper, A mobile robotic chemist, *Nature*, 2020, **583**, 237–241.

21 T. Dai, S. Vijayakrishnan, F. T. Szczypiński, J.-F. Ayme, E. Simaei, T. Fellowes, R. Clowes, L. Kotopanov, C. E. Shields, Z. Zhou, J. W. Ward and A. I. Cooper, Autonomous mobile robots for exploratory synthetic chemistry, *Nature*, 2024, **635**, 890–897.

22 I. W. Ashworth, L. Frodsham, P. Moore and T. O. Ronson, Evidence of rate-limiting proton transfer in an SNAr aminolysis in acetonitrile under synthetically relevant conditions, *J. Org. Chem.*, 2021, **87**, 2111–2119.

23 X. Zhao, N. J. Webb, M. P. Muehlfeld, A. L. Stottlemyer and M. W. Russell, Application of a semiautomated crystallizer to study oiling-out and agglomeration events—A case study in industrial crystallization optimization, *Org. Process Res. Dev.*, 2021, **25**, 564–575.

24 J. A. Jurica and J. P. McMullen, Automation technologies to enable data-rich experimentation: Beyond design of experiments for process modeling in late-stage process development, *Org. Process Res. Dev.*, 2021, **25**, 282–291.

25 A. M. Lunt, H. Fakhruldeen, G. Pizzuto, L. Longley, A. White, N. Rankin, R. Clowes, B. Alston, L. Gigli, G. M. Day, A. I. Cooper and S. Y. Chong, Modular, multi-robot integration of laboratories: an autonomous workflow for solid-state chemistry, *Chem. Sci.*, 2024, **15**, 2456–2463.

26 Q. Zhu, F. Zhang, Y. Huang, H. Xiao, L. Zhao, X. Zhang, T. Song, X. Tang, X. Li, G. He, B. Chong, J. Zhou, Y. Zhang, B. Zhang, J. Cao, M. Luo, S. Wang, G. Ye, W. Zhang, X. Chen, S. Cong, D. Zhou, H. Li, J. Li, G. Zou, W. Shang and J. Jiang, An all-round AI-Chemist with a scientific mind, *Natl. Sci. Rev.*, 2022, **9**, nwac190.

27 Q. Zhu, Y. Huang, D. Zhou, L. Zhao, L. Guo, R. Yang, Z. Sun, M. Luo, F. Zhang, H. Xiao, X. Tang, X. Zhang, T. Song, X. Li, B. Chong, J. Zhou, Y. Zhang, B. Zhang, J. Cao, G. Zhang, S. Wang, G. Ye, W. Zhang, H. Zhao, S. Cong, H. Li, L. Ling, Z. Zhang, W. Shang and J. Jiang, Automated synthesis of oxygen-producing catalysts from Martian meteorites by a robotic AI chemist, *Nat. Synth.*, 2024, **3**, 319–328.

28 N. J. Szymanski, B. Rendy, Y. Fei, R. E. Kumar, T. He, D. Milsted, M. J. McDermott, M. Gallant, E. D. Cubuk, A. Merchant, H. Kim, A. Jain, C. J. Bartel, K. Persson, Y. Zeng and G. Ceder, An autonomous laboratory for the accelerated synthesis of novel materials, *Nature*, 2023, **624**, 86–91.

29 H. Zhao, W. Chen, H. Huang, Z. Sun, Z. Chen, L. Wu, B. Zhang, F. Lai, Z. Wang, M. L. Adam, C. H. Pang, P. K. Chu, Y. Lu, T. Wu, J. Jiang, Z. Yin and X.-F. Yu, A robotic platform for the synthesis of colloidal nanocrystals, *Nat. Synth.*, 2023, **2**, 505–514.

30 T. Ha, D. Lee, Y. Kwon, M. S. Park, S. Lee, J. Jang, B. Choi, H. Jeon, J. Kim, H. Choi, H.-T. Seo, W. Choi, W. Hong, Y. J. Park, J. Jang, J. Cho, B. Kim, H. Kwon, G. Kim, W. S. Oh, J. W. Kim, J. Choi, M. Min, A. Jeon, Y. Jung, E. Kim, H. Lee and Y.-S. Choi, AI-driven robotic chemist for autonomous synthesis of organic molecules, *Sci. Adv.*, 2023, **9**, eadj0461.

31 H. Fakhruldeen, G. Pizzuto, J. Glowacki and A. I. Cooper, ARChemist: Autonomous robotic chemistry system architecture, *arXiv*, 2022, **2204**, 13571.

32 Cronin group, *Pylabware*, 2021. Available from: https://github.com/croningp/pylabware.

33 M. Quigley, B. Gerkey, K. Conley, J. Faust, T. Foote, J. Leibs, E. Berger, R. Wheeler and A. Y. Ng, ROS: an open-source robot operating system, in *Proceedings of the open-source software workshop at the international conference on robotics and automation*, 2009.

34 W. Jia, T. Yang and X. Zhang, The rise of robots and the fall of cost stickiness: Evidence from Chinese manufacturers, *Account. Finance*, 2023, **63**, 3147–3171.

35 W. Zhang, M. A. Guy, J. Yang, L. Hao, J. Liu, J. M. Hawkins, J. Mustakis, S. Monfette and J. E. Hein, Leveraging GPT-4 to transform chemistry from paper to practice, *Digital Discovery*, 2024, **3**, 2367–2376.

36 M. Mc Mahon, *Pywinauto, version 0.6.6*, 2018. Available from: https://github.com/pywinauto/pywinauto.

37 P. H. C. Eilers and H. F. M. Boelens , *Baseline correction with asymmetric least squares smoothing*. Leiden University Medical Centre Report, 2005, 1, 5.